Supporting Information

Neutral Radical and Singlet Biradical Forms of meso-Free, Keto, and Diketo Hexaphyrins(1.1.1.1.1.1): Effects on Aromaticity and Photophysical Properties

Masatoshi Ishida,[†] *Jae-Yoon Shin,*[†] *Jong Min Lim,*[†] *Byung Sun Lee,*[†] *Min-Chul Yoon,*[†] *Taro Koide,*[‡] *Jonathan L. Sessler,**[§,†] *Atsuhiro Osuka*[*,‡] *and Dongho Kim*[*,†]

[†]Spectroscopy Laboratory for Functional π-Electronic Systems and Department of Chemistry, Yonsei University, Seoul 120-749, Korea,

[‡]Department of Chemistry, Graduate School of Science, Kyoto University, Sakyo-ku, Kyoto 606-8502, Japan,

[§]Department of Chemistry and Biochemistry, The University of Texas at Austin, 1 University Station – A5300, Austin, Texas 78712-0165, USA

Table of Contents

Scheme S1. Possible canonical resonance structures of **3**.

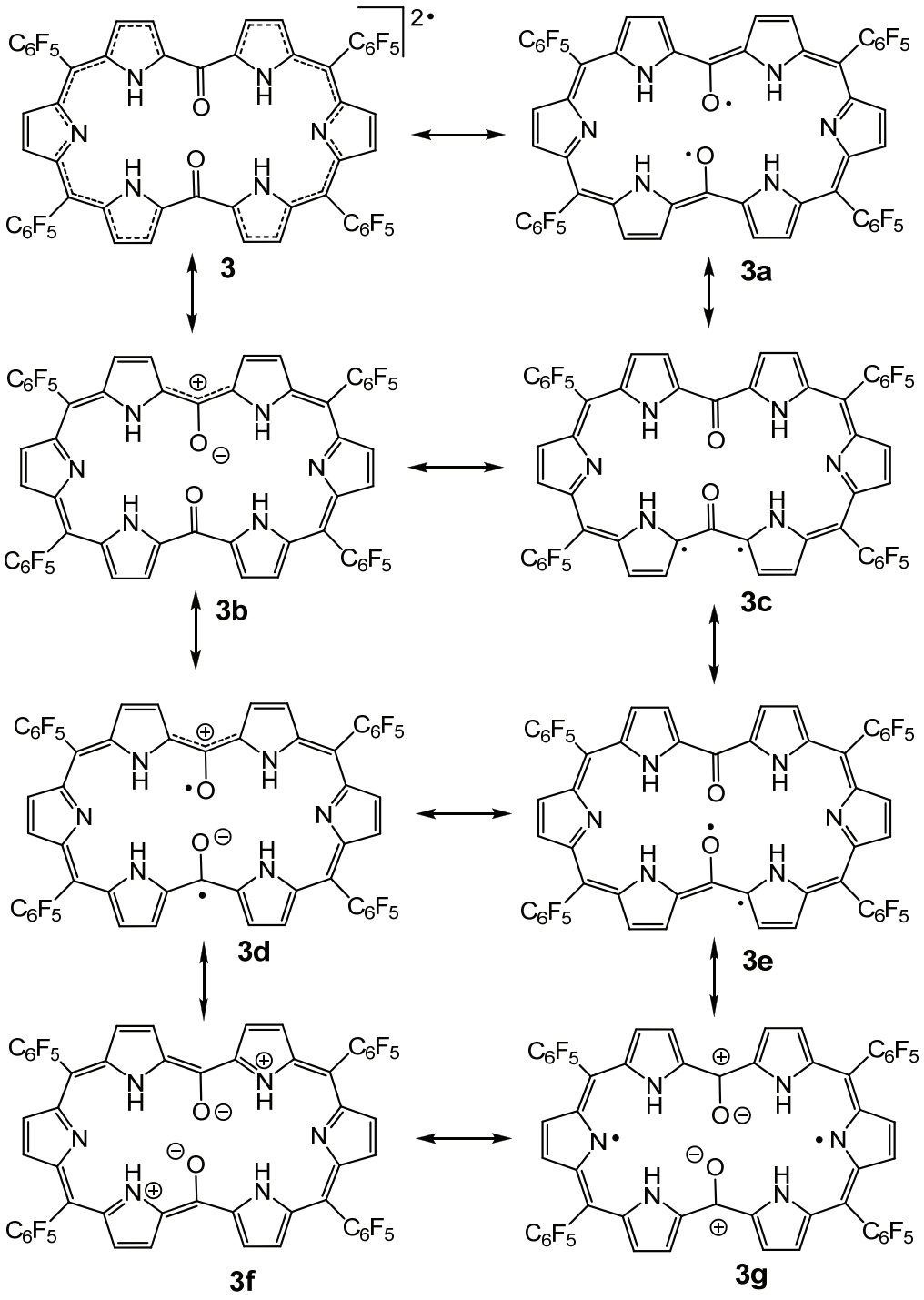

Table S1. Comparison of the crystal structural data of the core unit with that of the theoretical optimized structure for **1**. Selected Bond lengths (BLs, Å) and angles (BAs, °) are shown with the numbered atoms in the figure below. The data of the optimized structures in the table were obtained from DFT calculations of **1** carried out at the B3LPY/6-31G(d,p) level.

BLs and BAs	**1**(x-ray)	**1**(opt)	BLs and BAs	**1**(x-ray)	**1**(opt)
C(1)-C(2)	1.455	1.464	C(26)-C(27)	1.431	1.435
C(2)-C(3)	1.344	1.352	C(27)-C(28)	1.363	1.367
C(3)-C(4)	1.464	1.468	C(28)-C(29)	1.430	1.435
C(4)-C(5)	1.396	1.402	C(29)-C(30)	1.396	1.406
C(5)-C(6)	1.396	1.402	C(30)-C(1)	1.403	1.410
C(6)-C(7)	1.463	1.468	C(1)-N(1)	1.358	1.355
C(7)-C(8)	1.388	1.352	N(1)-C(4)	1.367	1.364
C(8)-C(9)	1.456	1.464	C(6)-N(2)	1.362	1.364
C(9)-C(10)	1.407	1.410	N(2)-C(9)	1.360	1.355
C(10)-C(11)	1.392	1.406	C(11)-N(3)	1.367	1.374
C(11)-C(12)	1.413	1.435	N(3)-C(14)	1.389	1.374
C(12)-C(13)	1.363	1.367	C(16)-N(4)	1.358	1.355
C(13)-C(14)	1.430	1.435	N(4)-C(19)	1.367	1.364
C(14)-C(15)	1.396	1.406	C(21)-N(5)	1.362	1.364
C(15)-C(16)	1.403	1.410	N(5)-C(24)	1.360	1.355
C(16)-C(17)	1.455	1.464	C(26)-N(6)	1.367	1.374
C(17)-C(18)	1.344	1.352	N(6)-C(29)	1.369	1.374
C(18)-C(19)	1.464	1.468	C(1)-N(1)-C(4)	105.78	106.03
C(19)-C(20)	1.396	1.402	C(6)-N(2)-C(9)	105.70	106.03
C(20)-C(21)	1.396	1.402	C(11)-N(3)-C(14)	109.67	110.19
C(21)-C(22)	1.463	1.468	C(16)-N(4)-C(19)	105.78	106.03
C(22)-C(23)	1.338	1.352	C(21)-N(5)-C(24)	105.70	106.03
C(23)-C(24)	1.456	1.464	C(26)-N(6)-C(29)	109.67	110.19
C(24)-C(25)	1.407	1.410			
C(25)-C(26)	1.392	1.406			

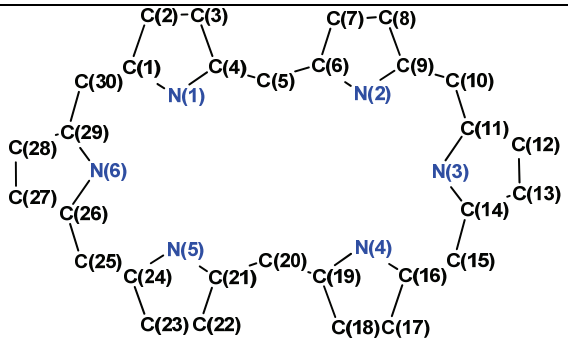

Table S2. Comparison of the crystal structural data of the core unit with that of the theoretical optimized structure for **2**. Selected Bond lengths (BLs, Å) and angles (BAs, °) are shown with the numbered atoms in the figure below. The data of the optimized structures in the table were obtained from DFT calculations of **2** carried out at the UB3LPY/6-31G(d,p) level.

BLs and BAs	**2**(x-ray)	**2**(opt)	BLs and BAs	**2**(x-ray)	**2**(opt)
C(1)-C(2)	1.419	1.436	C(26)-C(27)	1.461	1.447
C(2)-C(3)	1.357	1.371	C(27)-C(28)	1.351	1.345
C(3)-C(4)	1.410	1.434	C(28)-C(29)	1.464	1.457
C(4)-C(5)	1.402	1.394	C(29)-C(30)	1.420	1.396
C(5)-C(6)	1.415	1.394	C(30)-C(1)	1.406	1.409
C(6)-C(7)	1.416	1.430	C(1)-N(1)	1.368	1.353
C(7)-C(8)	1.364	1.373	N(1)-C(4)	1.386	1.381
C(8)-C(9)	1.420	1.435	C(6)-N(2)	1.385	1.378
C(9)-C(10)	1.407	1.406	N(2)-C(9)	1.370	1.364
C(10)-C(11)	1.404	1.420	C(11)-N(3)	1.359	1.368
C(11)-C(12)	1.459	1.464	N(3)-C(14)	1.385	1.371
C(12)-C(13)	1.342	1.350	C(16)-N(4)	1.365	1.357
C(13)-C(14)	1.460	1.461	N(4)-C(19)	1.366	1.377
C(14)-C(15)	1.404	1.395	C(21)-N(5)	1.371	1.376
C(15)-C(16)	1.406	1.430	N(5)-C(24)	1.368	1.362
C(16)-C(17)	1.418	1.415	C(26)-N(6)	1.385	1.375
C(17)-C(18)	1.373	1.395	N(6)-C(29)	1.356	1.365
C(18)-C(19)	1.409	1.406	C(20)-O(1)	1.248	1.281
C(19)-C(20)	1.416	1.458	C(1)-N(1)-C(4)	111.23	111.44
C(20)-C(21)	1.417	1.455	C(6)-N(2)-C(9)	111.28	111.03
C(21)-C(22)	1.412	1.405	C(11)-N(3)-C(14)	105.65	104.85
C(22)-C(23)	1.364	1.394	C(16)-N(4)-C(19)	110.85	111.30
C(23)-C(24)	1.409	1.413	C(21)-N(5)-C(24)	110.59	110.83
C(24)-C(25)	1.409	1.433	C(26)-N(6)-C(29)	105.76	105.58
C(25)-C(26)	1.395	1.393			

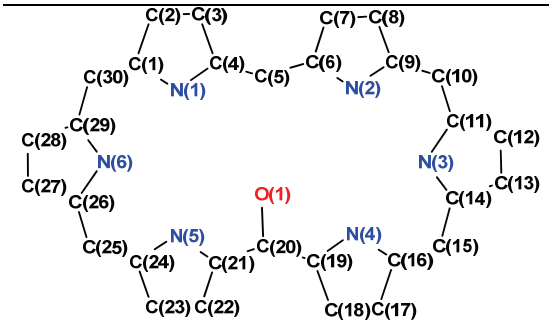

Table S3. Comparison of the crystal structural data of the core unit with that of the theoretical optimized structure for **3**. Selected Bond lengths (BLs, Å) and angles (BAs, °) are shown with the numbered atoms in the figure below. The data of the optimized structures in the table were obtained from DFT calculations of **3** carried out at the BS-UB3LPY/6-31G(d,p) level.

BLs and BAs	**3**(x-ray)	**3**(opt)	BLs and BAs	**3**(x-ray)	**3**(opt)
C(1)-C(2)	1.408	1.417	C(26)-C(27)	1.468	1.461
C(2)-C(3)	1.374	1.389	C(27)-C(28)	1.344	1.353
C(3)-C(4)	1.404	1.409	C(28)-C(29)	1.460	1.461
C(4)-C(5)	1.466	1.470	C(29)-C(30)	1.393	1.406
C(5)-C(6)	1.476	1.465	C(30)-C(1)	1.419	1.420
C(6)-C(7)	1.398	1.410	C(1)-N(1)	1.378	1.374
C(7)-C(8)	1.383	1.389	N(1)-C(4)	1.366	1.365
C(8)-C(9)	1.409	1.416	C(6)-N(2)	1.359	1.367
C(9)-C(10)	1.419	1.423	N(2)-C(9)	1.381	1.373
C(10)-C(11)	1.393	1.406	C(11)-N(3)	1.355	1.367
C(11)-C(12)	1.460	1.461	N(3)-C(14)	1.373	1.367
C(12)-C(13)	1.344	1.353	C(16)-N(4)	1.378	1.374
C(13)-C(14)	1.468	1.461	N(4)-C(19)	1.366	1.366
C(14)-C(15)	1.408	1.406	C(21)-N(5)	1.359	1.368
C(15)-C(16)	1.417	1.420	N(5)-C(24)	1.381	1.372
C(16)-C(17)	1.409	1.417	C(26)-N(6)	1.355	1.367
C(17)-C(18)	1.374	1.389	N(6)-C(29)	1.373	1.367
C(18)-C(19)	1.404	1.409	C(5)-O(1)	1.223	1.237
C(19)-C(20)	1.466	1.470	C(20)-O(2)	1.223	1.237
C(20)-C(21)	1.476	1.465	C(1)-N(1)-C(4)	110.92	110.48
C(21)-C(22)	1.398	1.409	C(6)-N(2)-C(9)	110.92	110.61
C(22)-C(23)	1.383	1.389	C(11)-N(3)-C(14)	105.29	105.58
C(23)-C(24)	1.409	1.416	C(16)-N(4)-C(19)	110.92	110.48
C(24)-C(25)	1.409	1.423	C(21)-N(5)-C(24)	110.92	110.61
C(25)-C(26)	1.393	1.406	C(26)-N(6)-C(29)	105.29	105.58

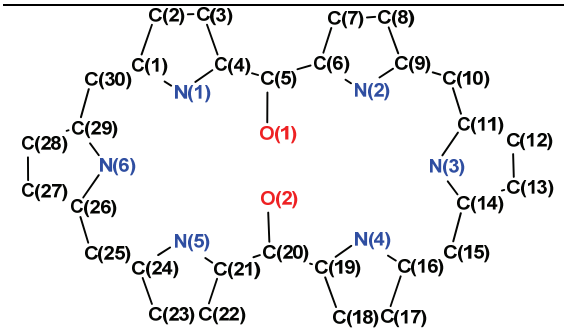

Table S4. Selected simulated excited states of **1** as inferred from TD-DFT analyses

Excited state	Transition Energy (eV, nm)	Oscillator strength (f)	CI transition	CI coefficient
1:	**1.4316 eV 866.04 nm**	**f=0.0399**	280 -> 283	-.47744
			281 -> 282	.56462
2:	**1.5911 eV 779.25 nm**	**f=0.0008**	280 -> 282	.48533
			281 -> 283	.52422
3:	**2.4495 eV 506.17 nm**	**f=0.9611**	277 -> 282	.12034
			280 -> 282	.39527
			281 -> 283	-.33444
4:	**2.4979 eV 496.36 nm**	**f=2.0807**	276 -> 282	.20060
			277 -> 283	-.13687
			280 -> 283	.42977
			281 -> 282	.26306
5:	**2.6254 eV 472.24 nm**	**f=0.0000**	278 -> 283	-.22045
			279 -> 282	.65500
6:	**2.7103 eV 457.46 nm**	**f=0.0000**	275 -> 282	.15091
			278 -> 282	.65186
			280 -> 284	-.12163
			281 -> 285	.10136
7:	**2.7597 eV 449.27 nm**	**f=0.0498**	277 -> 282	.67945
8:	**2.8824 eV 430.14 nm**	**f=0.0000**	278 -> 283	-.38306
			279 -> 282	-.12368
			280 -> 285	.11828
			281 -> 284	.56669
9:	**2.8869 eV 429.47 nm**	**f=0.0000**	275 -> 282	-.13492
			279 -> 283	.61473
			281 -> 285	.28646
10:	**3.0161 eV 411.08 nm**	**f=0.0706**	276 -> 282	.48615
			277 -> 283	.48082
11:	**3.0301 eV 409.18 nm**	**f=0.0000**	266 -> 282	.10215
			270 -> 282	-.13741
			275 -> 283	.17086
			278 -> 283	.49211
			279 -> 282	.10492
			280 -> 285	.24592
			281 -> 284	.30095
12:	**3.0523 eV 406.20 nm**	**f=0.8923**	276 -> 282	-.44319
			277 -> 283	.46988
			280 -> 283	.11245
			281 -> 282	.10607

Table S5. Selected simulated excited states of **2** as derived from TD-DFT calculations carried out at the UB3LYP/6-31G** level. Transitions A and B stand for the α-spin and β-spin.

Excited state	Transition Energy (eV, nm)	Oscillator strength (f)
CI transition	CI coefficient	
1:	**0.7156 eV 1732.61 nm**	**f=0.0061**
285A -> 288A	-.13931	
286A -> 287A	1.00029	
285B -> 286B	.31683	
2:	**1.1641 eV 1065.02 nm**	**f=0.1070**
285A -> 287A	-.38854	
286A -> 287A	-.15258	
286A -> 288A	.19837	
286A -> 289A	.18011	
284B -> 287B	-.24733	
285B -> 286B	.69606	
285B -> 287B	-.57285	
3:	**1.1693 eV 1060.32 nm**	**f=0.0776**
285A -> 287A	.44675	
286A -> 287A	-.11197	
286A -> 288A	-.25747	
286A -> 289A	.14874	
284B -> 287B	-.20587	
285B -> 286B	.59678	
285B -> 287B	.67155	
4:	**1.6206 eV 765.05 nm**	**f=0.0062**
285A -> 287A	-.11372	
286A -> 288A	.52699	
283B -> 287B	.10969	
284B -> 286B	.82411	
285B -> 287B	.33907	
5:	**1.7603 eV 704.34 nm**	**f=0.0024**
284A -> 287A	-.51497	
285A -> 288A	.20129	
286A -> 289A	.45432	
283B -> 286B	.17355	
284B -> 287B	.71720	
285B -> 288B	-.21178	
6:	**1.8431 eV 672.69 nm**	**f=0.0010**
285A -> 287A	.71179	
286A -> 288A	.63410	
284B -> 286B	-.19639	
285B -> 287B	-.23642	
7:	**2.1225 eV 584.15 nm**	**f=0.0494**
284A -> 287A	.59962	
286A -> 289A	.75406	
283B -> 286B	.19084	
284B -> 287B	-.13494	
285B -> 286B	-.12192	
8:	**2.2994 eV 539.20 nm**	**f=0.0322**
283A -> 287A	.45582	
284A -> 288A	.18427	
285A -> 289A	.41300	
282B -> 286B	.31243	
283B -> 287B	.54140	
284B -> 286B	-.16350	
284B -> 288B	.12415	
285B -> 289B	-.41795	
9:	**2.3327 eV 531.51 nm**	**f=0.0053**
284A -> 287A	-.19328	
285A -> 288A	.40573	
286A -> 289A	-.16574	
286A -> 290A	-.35847	
283B -> 286B	.51972	
284B -> 287B	-.40011	
285B -> 288B	-.44979	
10:	**2.3788 eV 521.20 nm**	**f=0.8006**
283A -> 287A	.12401	
285A -> 287A	.35145	
286A -> 288A	-.40725	
282B -> 286B	.15303	
283B -> 287B	.10238	
284B -> 286B	.46341	
285B -> 287B	-.28541	
285B -> 288B	.11592	
11:	**2.4336 eV 509.47 nm**	**f=0.0298**
282A -> 287A	.28025	
285A -> 288A	-.19885	
286A -> 290A	.17058	
281B -> 286B	.21922	
282B -> 287B	.47251	
283B -> 286B	.61615	
285B -> 288B	.39009	
12:	**2.5388 eV 488.35 nm**	**f=0.0073**
281A -> 287A	.26793	
282A -> 288A	-.10795	
285A -> 289A	-.15061	
281B -> 287B	.38495	
282B -> 286B	.76692	
285B -> 289B	.32639	
13:	**2.5790 eV 480.75 nm**	**f=0.6676**
281A -> 288A	-.10363	
282A -> 287A	.19878	
284A -> 287A	.45298	
284A -> 289A	.13557	
285A -> 288A	.47889	
286A -> 289A	-.25483	
281B -> 286B	.21239	
281B -> 288B	.10261	
282B -> 287B	.26499	
283B -> 286B	-.12960	
284B -> 287B	.35423	
285B -> 288B	-.12940	
14:	**2.6241 eV 472.49 nm**	**f=0.3503**
281A -> 288A	.16530	
282A -> 287A	-.39520	
283A -> 288A	.11730	
284A -> 287A	.22993	
285A -> 288A	.17688	
286A -> 289A	-.16485	
276B -> 287B	-.10690	
281B -> 286B	-.21294	
281B -> 288B	-.12645	
282B -> 287B	-.35294	
283B -> 286B	.40239	
284B -> 287B	.22636	
284B -> 289B	-.16524	
285B -> 288B	.41832	

Table S6. Selected simulated excited states of **3** as derived from TD-DFT calculations carried out at the UB3LYP/6-31G** level. Transitions A and B stand for the α-spin and β-spin,

Excited state	Transition Energy (eV, nm)	Oscillator strength (f)
CI transition	CI coefficient	
1:	**0.9282 eV 1335.73 nm**	**f=0.0000**
289A -> 290A	.73895	
289B -> 290B	.73894	
2:	**1.1899 eV 1041.99 nm**	**f=0.2375**
288A -> 291A	-.11927	
289A -> 290A	-.64979	
288B -> 291B	.11927	
289B -> 290B	.64979	
3:	**1.3187 eV 940.17 nm**	**f=0.0000**
287A -> 290A	.15617	
288A -> 290A	.15645	
289A -> 291A	.71732	
287B -> 290B	.15617	
288B -> 290B	.15645	
289B -> 291B	.71732	
4:	**1.4534 eV 853.05 nm**	**f=0.0100**
287A -> 290A	.20660	
288A -> 290A	.42066	
289A -> 291A	-.55060	
289A -> 292A	.18892	
287B -> 290B	-.20660	
288B -> 290B	-.42066	
289B -> 291B	.55061	
289B -> 292B	-.18892	
5:	**1.5812 eV 784.12 nm**	**f=0.0000**
288A -> 290A	.70200	
289A -> 291A	-.17159	
289A -> 292A	-.12848	
288B -> 290B	.70200	
289B -> 291B	-.17158	
289B -> 292B	-.12848	
6:	**2.1643 eV 572.87 nm**	**f=0.0155**
287A -> 290A	.47307	
289A -> 291A	.22967	
289A -> 292A	.45503	
287B -> 290B	-.47306	
289B -> 291B	-.22968	
289B -> 292B	-.45503	
7:	**2.2102 eV 560.96 nm**	**f=0.0000**
286A -> 290A	.24531	
287A -> 291A	-.14175	
287A -> 292A	.19119	
288A -> 291A	.64098	
286B -> 290B	.24532	
287B -> 291B	-.14174	
287B -> 292B	.19119	
288B -> 291B	.64098	
8:	**2.2567 eV 549.41 nm**	**f=0.0575**
286A -> 290A	.53924	
287A -> 290A	-.19767	
287A -> 291A	.24246	
288A -> 290A	.20833	
288A -> 292A	.13272	
289A -> 291A	.10205	
289A -> 293A	.16782	
286B -> 290B	-.53923	
287B -> 290B	.19766	
287B -> 291B	-.24246	
288B -> 290B	-.20833	
288B -> 292B	-.13272	
289B -> 291B	-.10205	
289B -> 293B	-.16782	
9:	**2.2612 eV 548.31 nm**	**f=0.1374**
286A -> 290A	.28098	
287A -> 290A	.31613	
287A -> 291A	.13550	
288A -> 290A	-.36319	
289A -> 291A	-.22232	
289A -> 292A	-.26489	
286B -> 290B	-.28097	
287B -> 290B	-.31612	
287B -> 291B	-.13550	
288B -> 290B	.36319	
289B -> 291B	.22232	
289B -> 292B	.26488	
10:	**2.3220 eV 533.95 nm**	**f=0.0000**
287A -> 290A	.59661	
288A -> 290A	-.14251	
289A -> 291A	-.10329	
289A -> 292A	-.31687	
287B -> 290B	.59662	
288B -> 290B	-.14252	
289B -> 291B	-.10330	
289B -> 292B	-.31687	
11:	**2.3616 eV 525.01 nm**	**f=0.0000**
285A -> 290A	.13334	
286A -> 290A	.62689	
288A -> 291A	-.25233	
285B -> 290B	.13334	
286B -> 290B	.62690	
288B -> 291B	-.25233	
12:	**2.4081 eV 514.87 nm**	**f=0.6134**
287A -> 290A	-.29875	
287A -> 291A	.17687	
288A -> 290A	-.27082	
289A -> 291A	-.15657	
289A -> 292A	.40028	
287B -> 290B	.29875	
287B -> 291B	-.17687	
288B -> 290B	.27082	
289B -> 291B	.15657	
289B -> 292B	-.40026	
13:	**2.4525 eV 505.53 nm**	**f=0.0918**
286A -> 290A	-.30860	
287A -> 291A	.50396	
288A -> 292A	.26517	
289A -> 292A	-.13391	
289A -> 293A	.13272	
286B -> 290B	.30860	
287B -> 291B	-.50396	
288B -> 292B	-.26517	
289B -> 292B	.13389	
289B -> 293B	-.13272	

Table S7. HOMA values of the full structures of **1, 2** and **3**, along with their π-conjugated pathways. The values were obtained using of the geometries of the X-ray crystal structural data and that of optimizations carried out at the RB3LPY/6-31G(d, p) the level for **1**, UB3LPY/6-31G(d, p) level for **2** and the BS-UB3LYP/6-31G(d, p) level for **3**, respectively.

Compound	HOMA[a]	EN	GEO
1 (Opt)[b]	0.844	0.090	0.066
1 (X-ray)[c]	0.890	0.050	0.061
2 (Opt) [b]	0.731	0.156	0.113
2 (X-ray) [c]	0.875	0.052	0.073
3 (Opt) [b]	0.672	0.144	0.185
3 (X-ray) [c]	0.680	0.131	0.189

a) HOMA = 1 – EN – GEO = 1 – [$\alpha(R_{opt} - R_{av})^2 + \frac{\alpha}{n}\sum(R_{opt} - R_i)^2$] where α is an empirical constant chosen to give HOMA = 0 for the hypothetical Kekulé structure and HOMA = 1 for a system with all bonds equal to an optimal bond length R_{opt}, n is the number of bonds in the summation, and R_{av} is an averaged bond length of R_i, where R_i is the heteroatom-corrected bond length of the *i* th bond in the π-conjugated pathway. The EN term in this equation describes changes in the aromatic character due to deviations of the average bond length away from the optimal value, while the GEO term reflects the consequences of bond-length alteration.

b) The value was determined using the optimized structural data

c) The value was derived from the X-ray crystallographic data [9a, b].

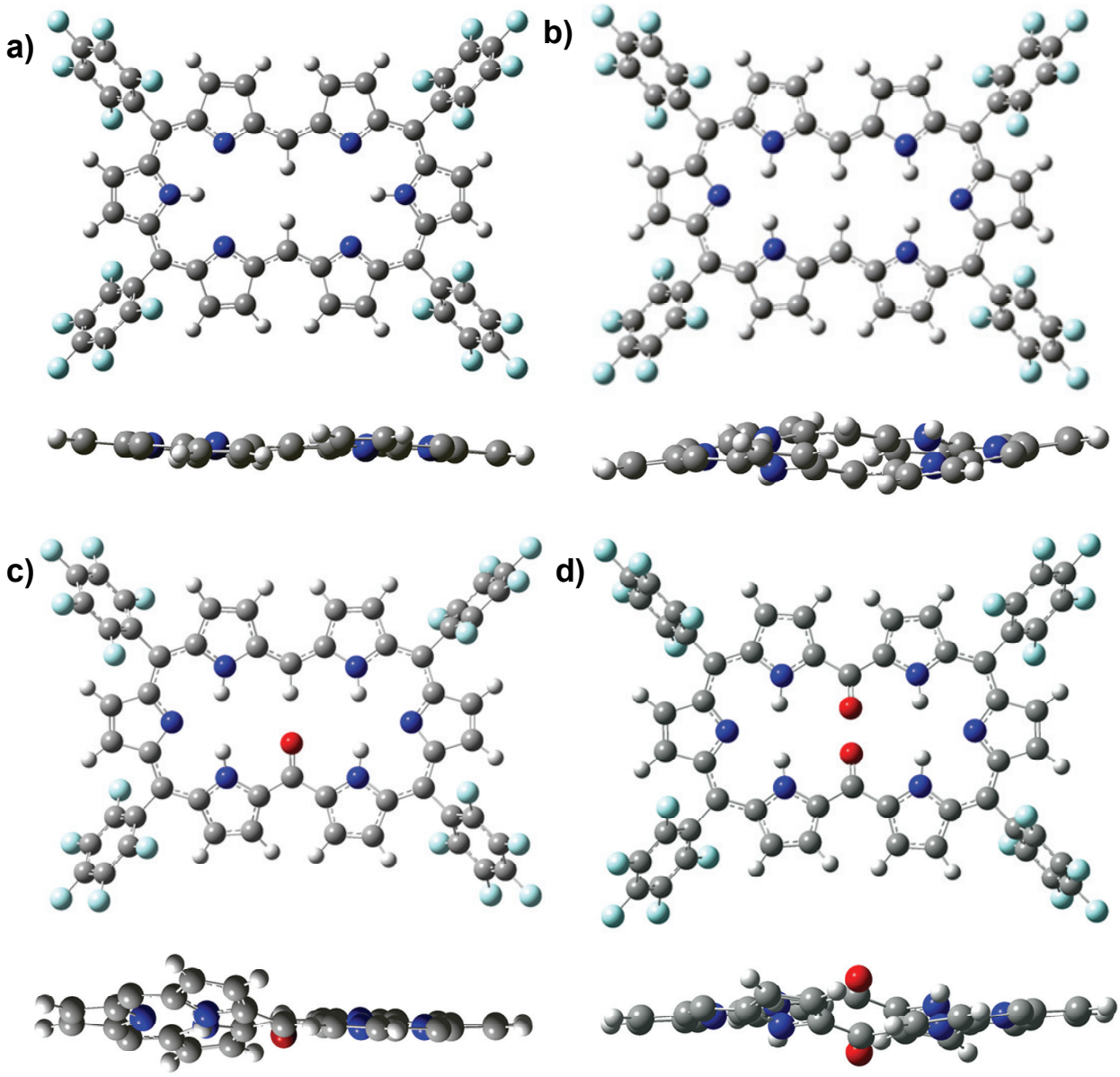

Figure S1. Optimized structures of (a) **1**, (b) **4**, (c) **2** and (d) **3** calculated at the (U)B3LYP/6-31G(d,p) level. The top view (above) and side view (bottom) of the resulting models are shown. The meso-aryl substituents of the derivative in question have been omitted for clarity in the side views.

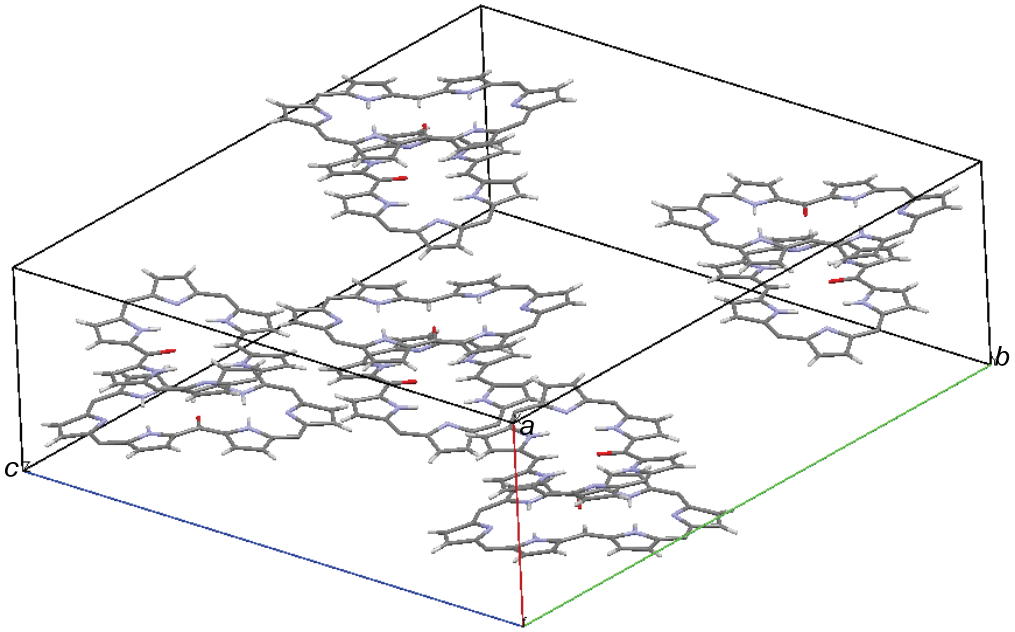

Figure S2. Crystal packing diagram of **2** with the structure shown in stick model form. This structure was first reported in ref 9a. In this view, the meso pentafluorophenyl groups are omitted for clarity. Various intermolecular interactions are found in the crystal packing of **2** in which each of dimers is separated by ca. 3.5 Å and oriented in a nearly perpendicular manner. This result provides support for the antiferromagnetic coupling inferred from the temperature dependent magnetic susceptibility measurements carried out in the solid state. Intermolecular π-radical interactions similar to those proposed here are typical features seen in neutral phenalenyl radicals with planar geometry (Reference: Suzuki, S.; Morita, Y.; Fukui, K.; Sato, K.; Shiomi, D.; Takui, T.; Nakasuji, K. *J. Am. Chem. Soc.* **2006**, *128*, 2530.).

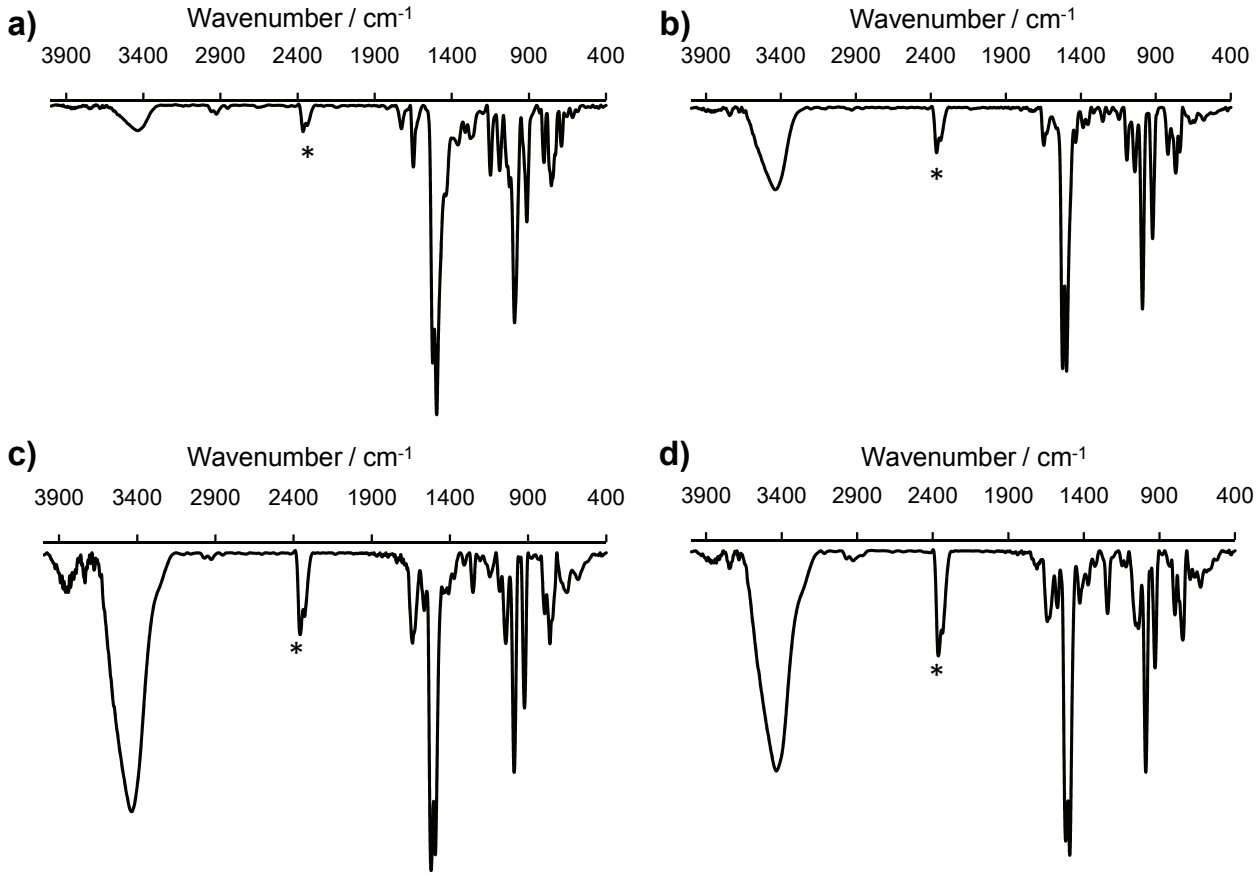

Figure S3. FTIR spectra of (a) **5** (b) **1**, (c) **2** and (d) **3** recorded in a KBr pellet. The asterisk shows peaks arising from CO_2 present as a contaminant.

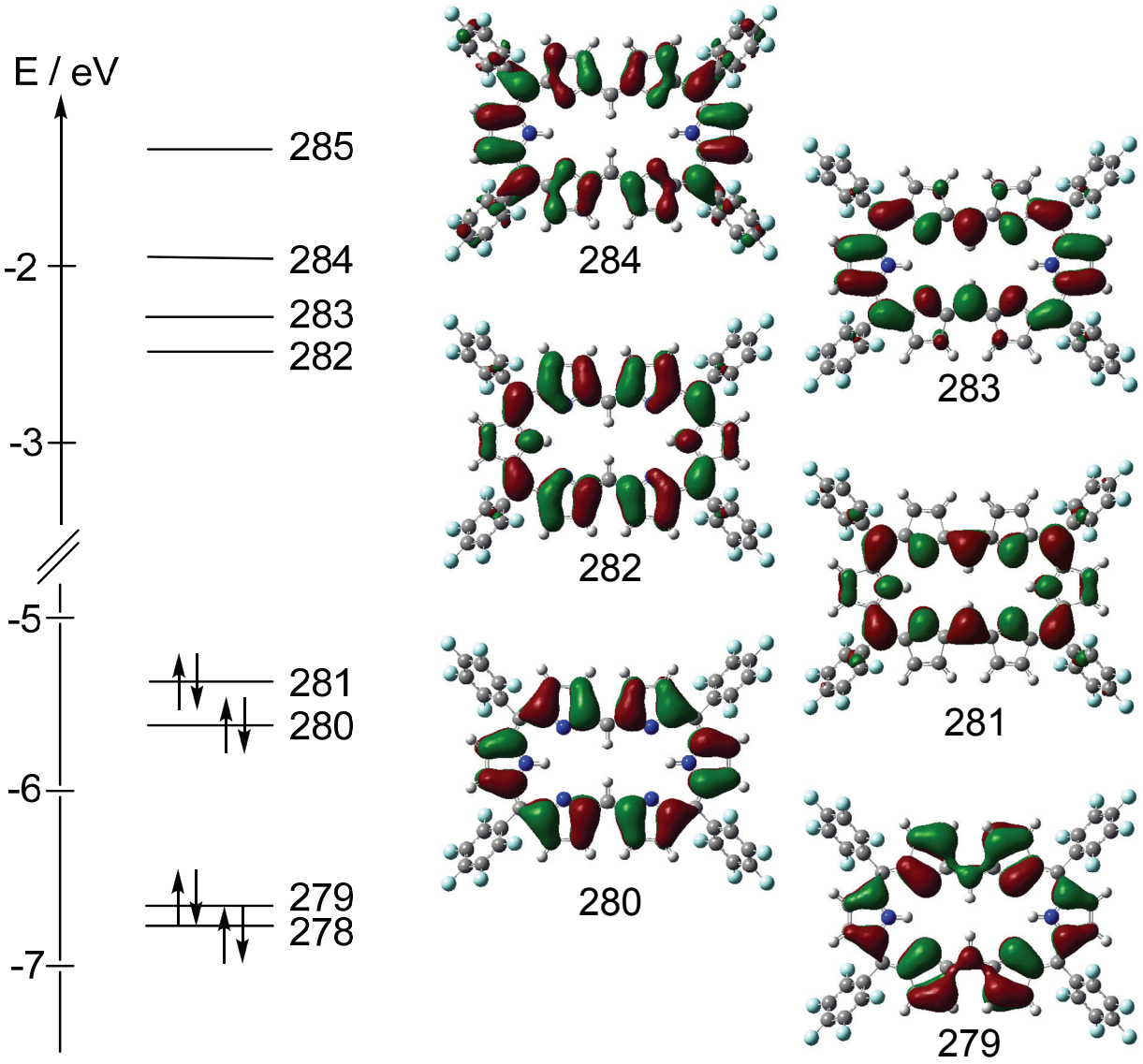

Figure S4. Calculated MO energy levels and energy diagrams for **1** as derived from analyses carried out at the B3LYP/6-31G** level.

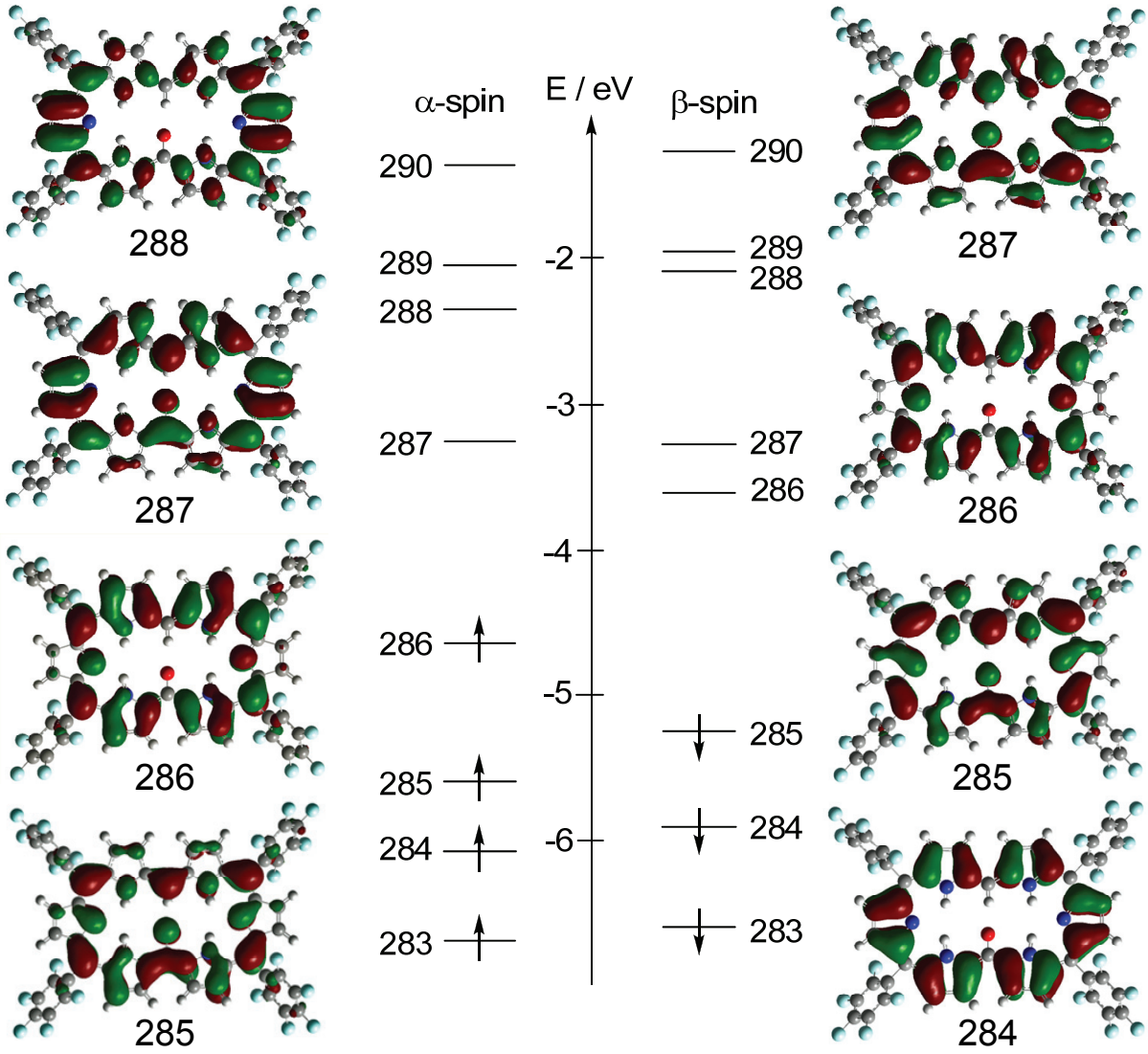

Figure S5. Calculated MO levels and energy diagrams for **2** from analyses carried out at the UB3LYP/6-31G** level.

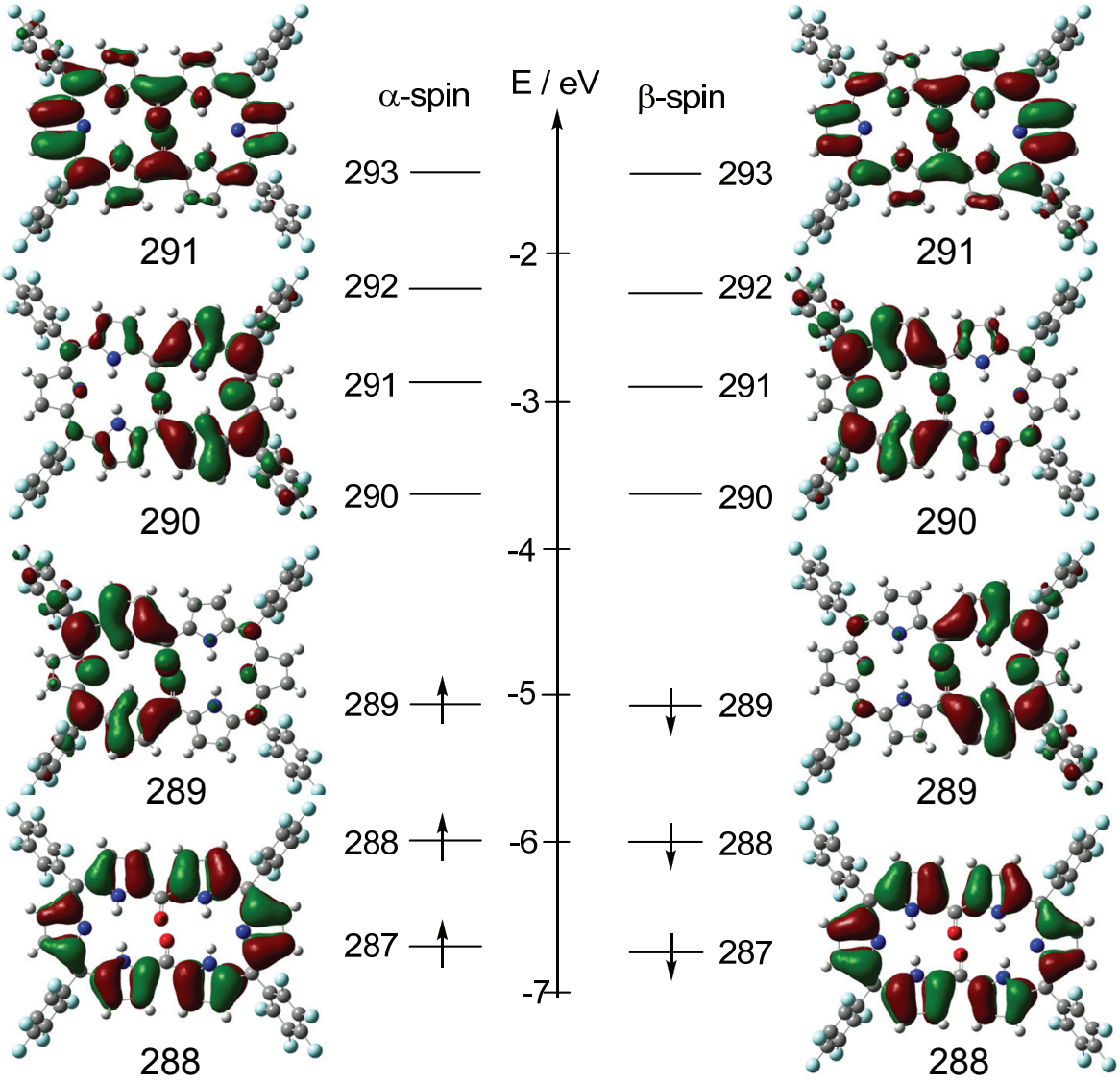

Figure S6. Calculated MO levels and energy diagrams for **3** derived from analyses carried out at the BS-UB3LYP/6-31G** level.

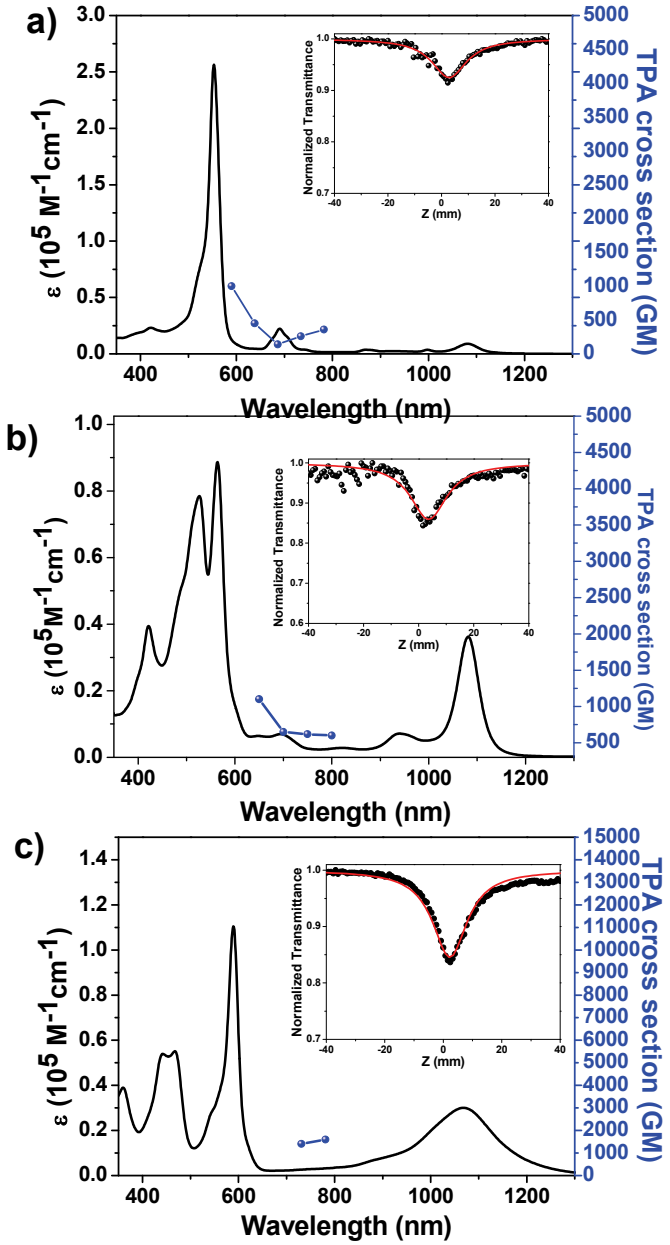

Figure S7. Two-photon absorption spectra and z-scan traces (inset) of (a) **1**, (b) **2**, and (c) **3** recorded in toluene using an excitation wavelength of 1600 nm.

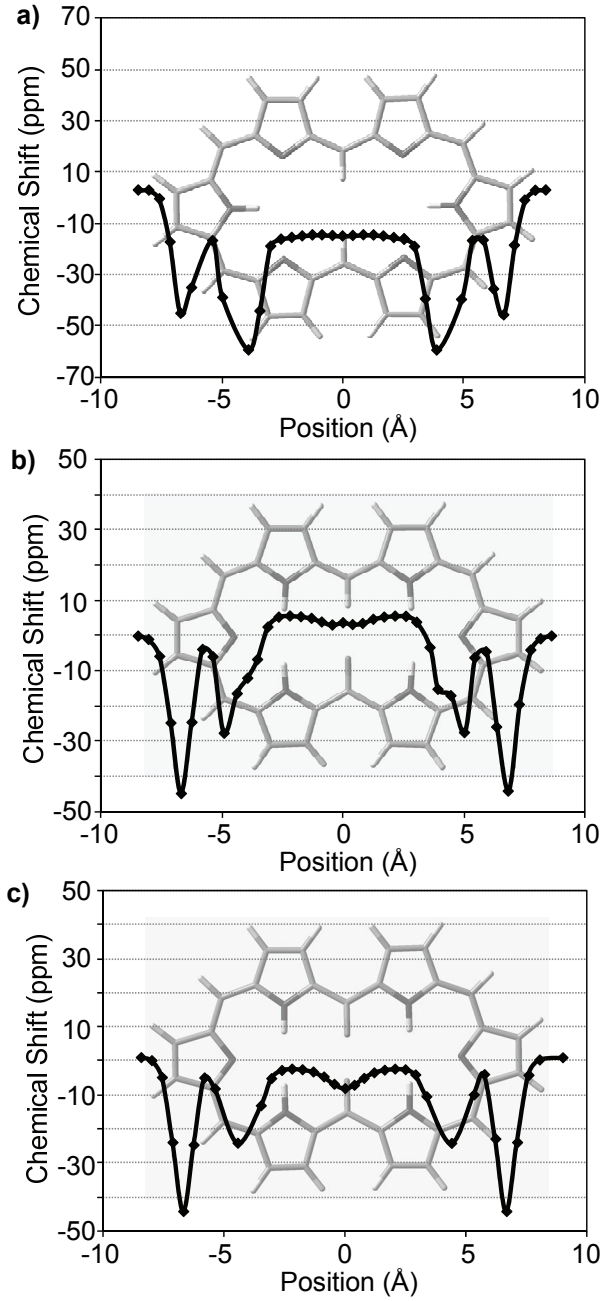

Figure S8. Transverse NICS scan spectra of (a) **1**, (b) **2** and (c) **3**. The meso pentafluorophenyl substituents have beren omitted for clarity. Selected NICS(0) values were calculated at zero height and within the hexaphyrin macrocyclic planes. These calculations were carried out at the (U)B3LYP/6-31G(d,p) level.

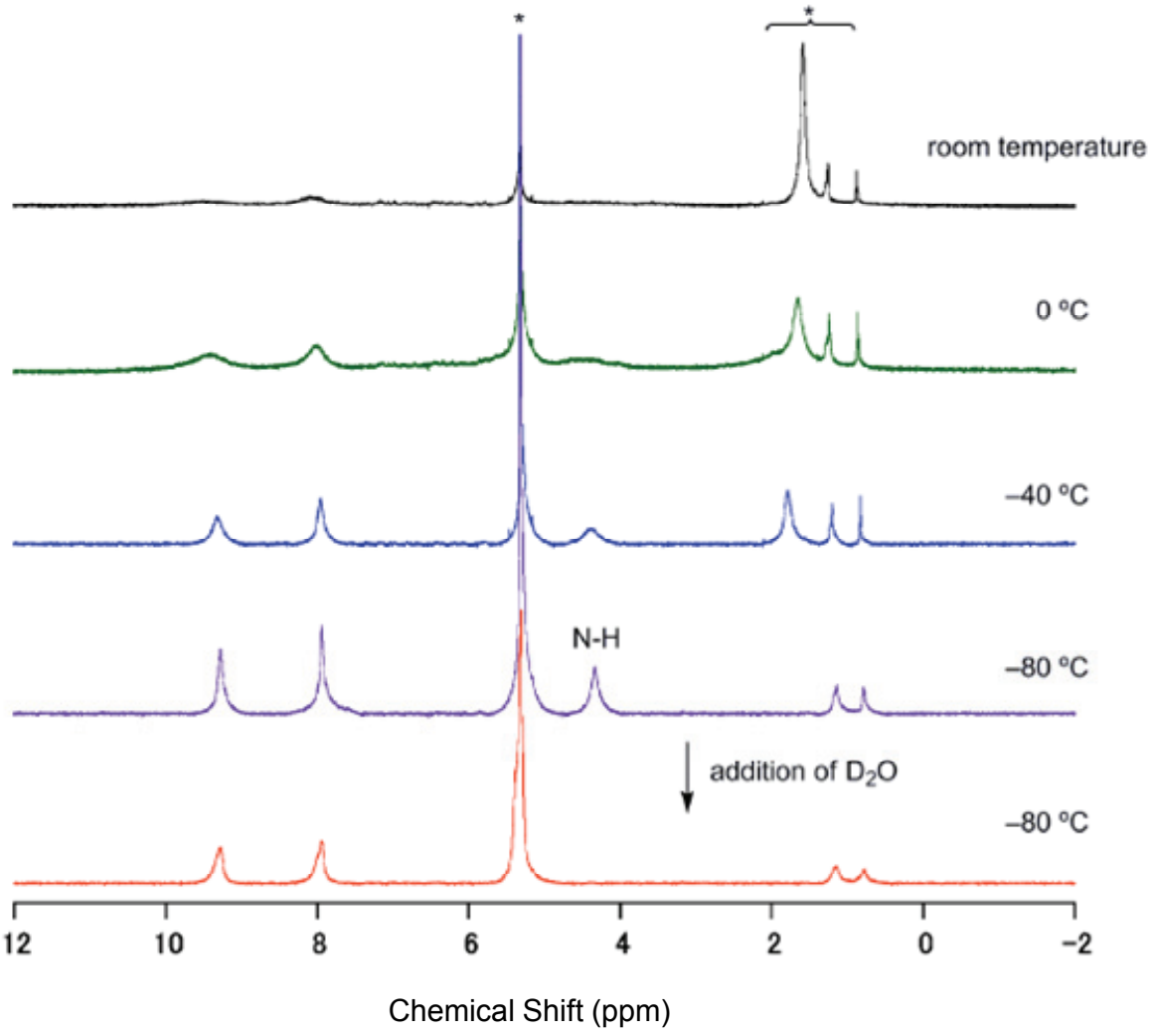

Figure S9. Variable temperature ^{1}H-NMR spectra of **3** recorded in CD_2Cl_2. An asterisk is used to denote the residual solvent and signals originating from impurities.

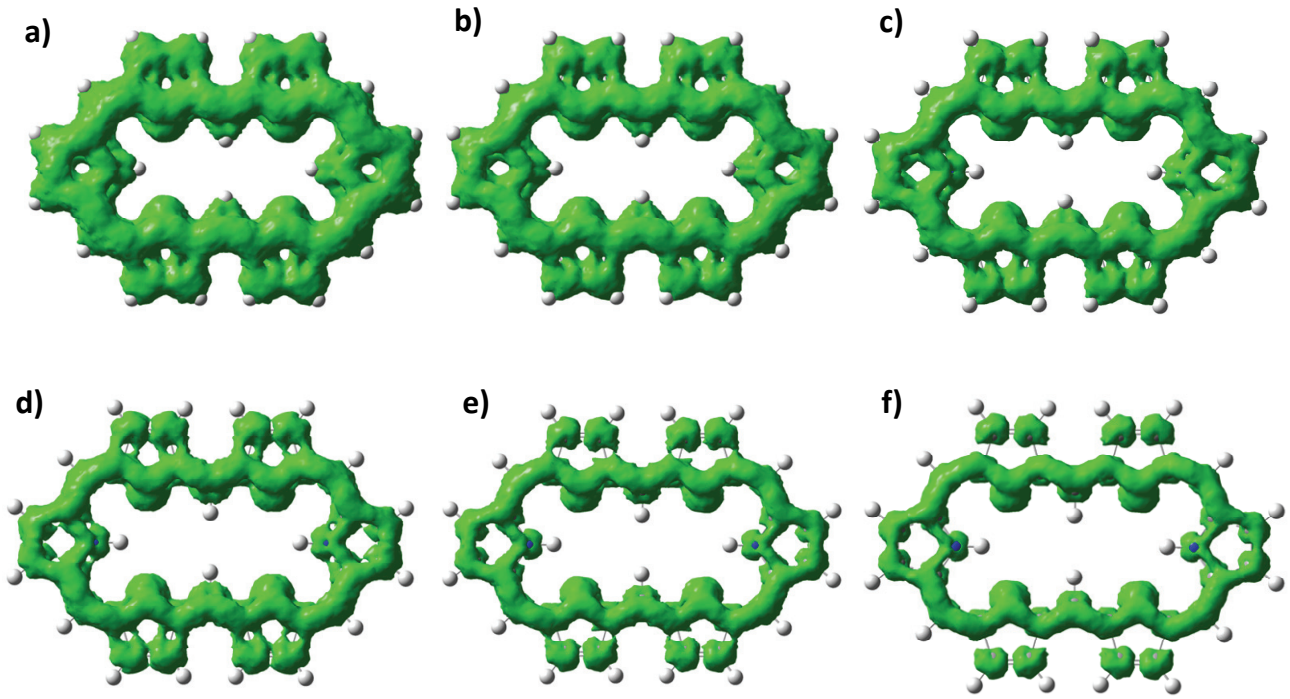

Figure S10. AICD plots of **1** with isosurface values of a) 0.03, b) 0.04, c) 0.05, d) 0.06, e) 0.07 and f) 0.08, respectively.

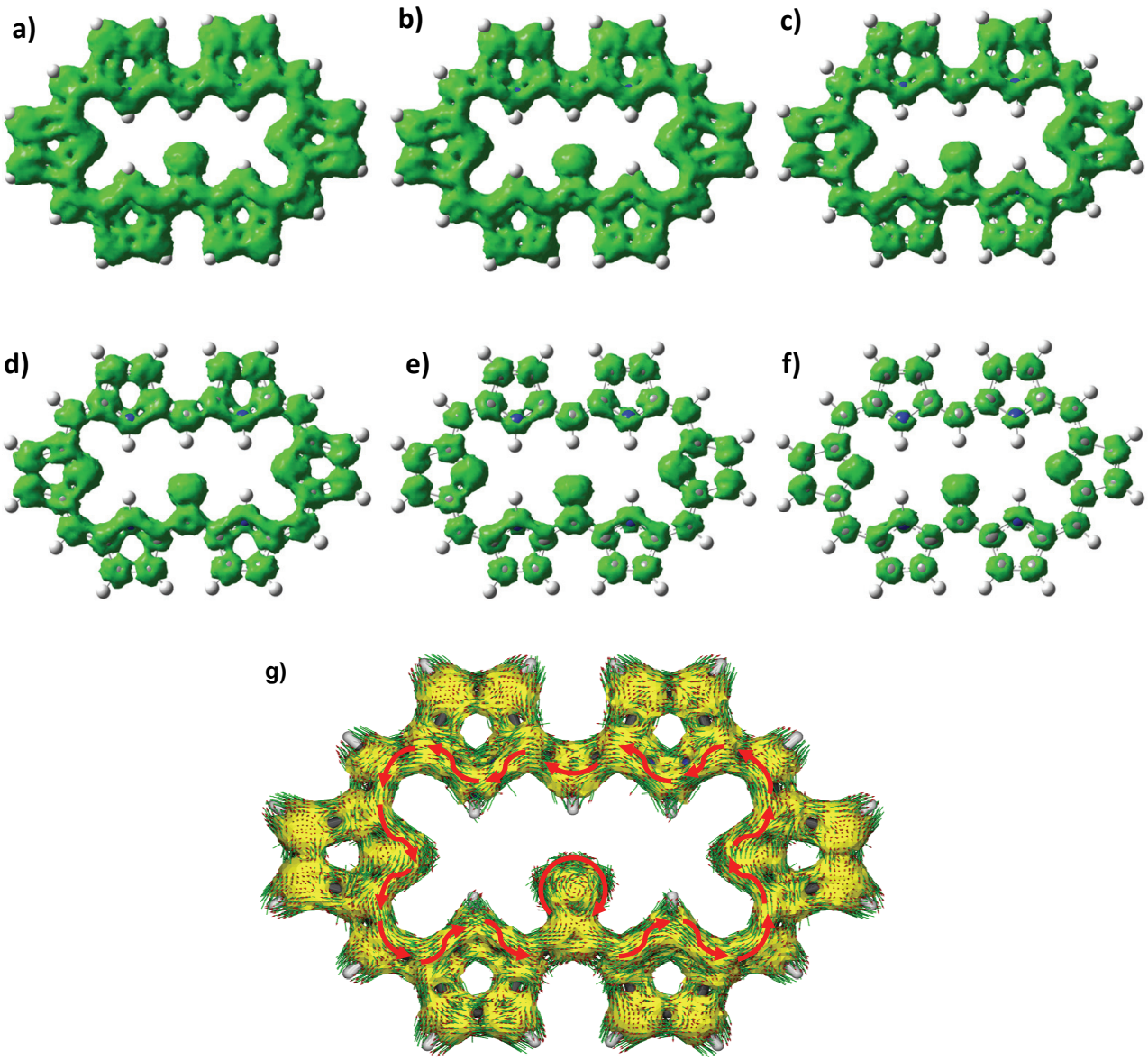

Figure S11. AICD plots of **2** with isosurface values of a) 0.03, b) 0.04, c) 0.05, d) 0.06, e) 0.07 and f) 0.08, respectively. (g) The illustrated red (counter-clockwise) vectors represent the direction of the overall ring currents when viewed in the direction opposite to that of the magnetic field vector.

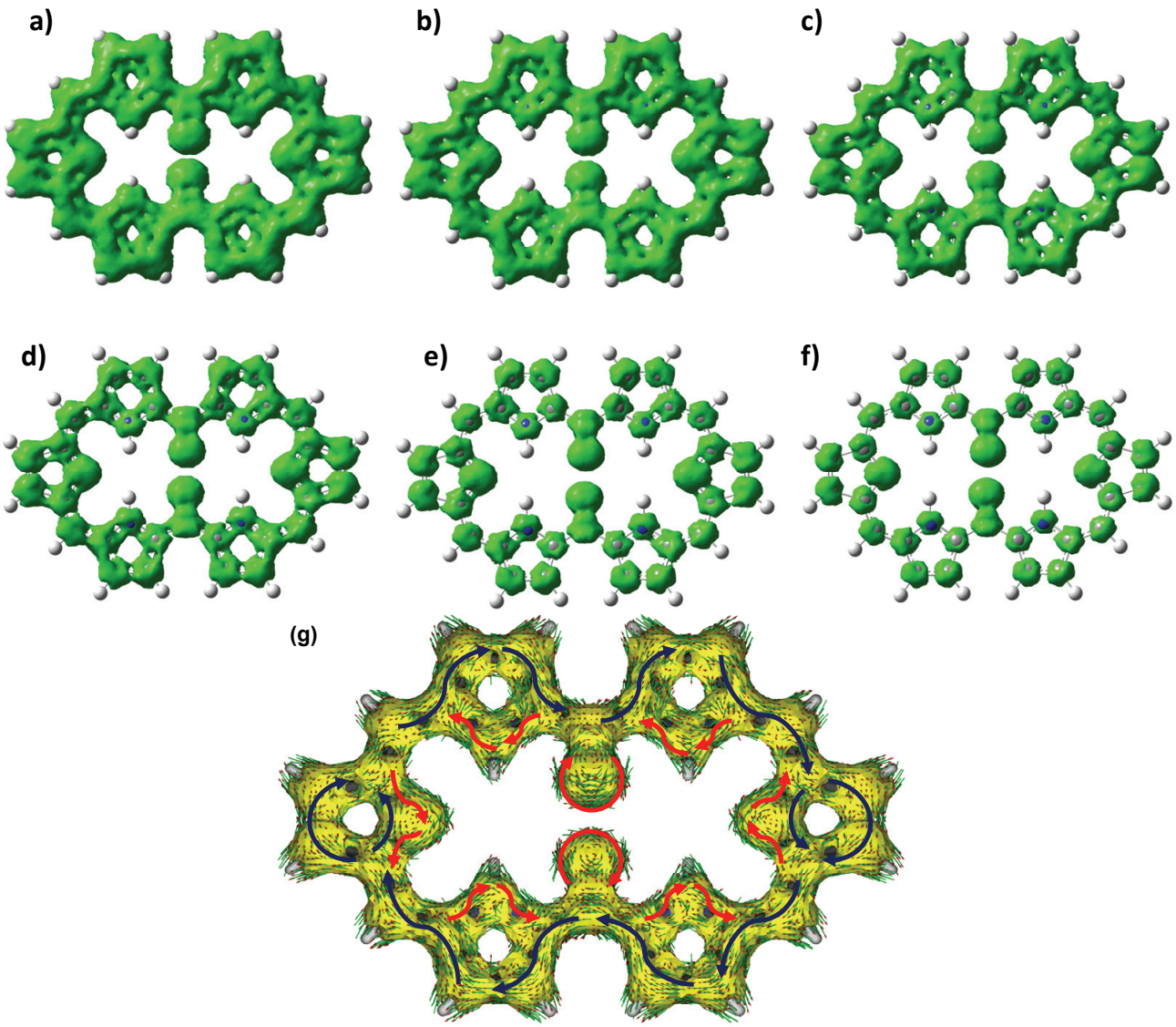

Figure S12. AICD plots of **3** with isosurface values of a) 0.03, b) 0.04, c) 0.05, d) 0.06, e) 0.07 and f) 0.08, respectively. (g) The illustrated blue (clockwise) and red (counter-clockwise) vectors represent each of the direction of the overall ring currents, respectively, when viewed in the direction opposite to that of the magnetic field vector.

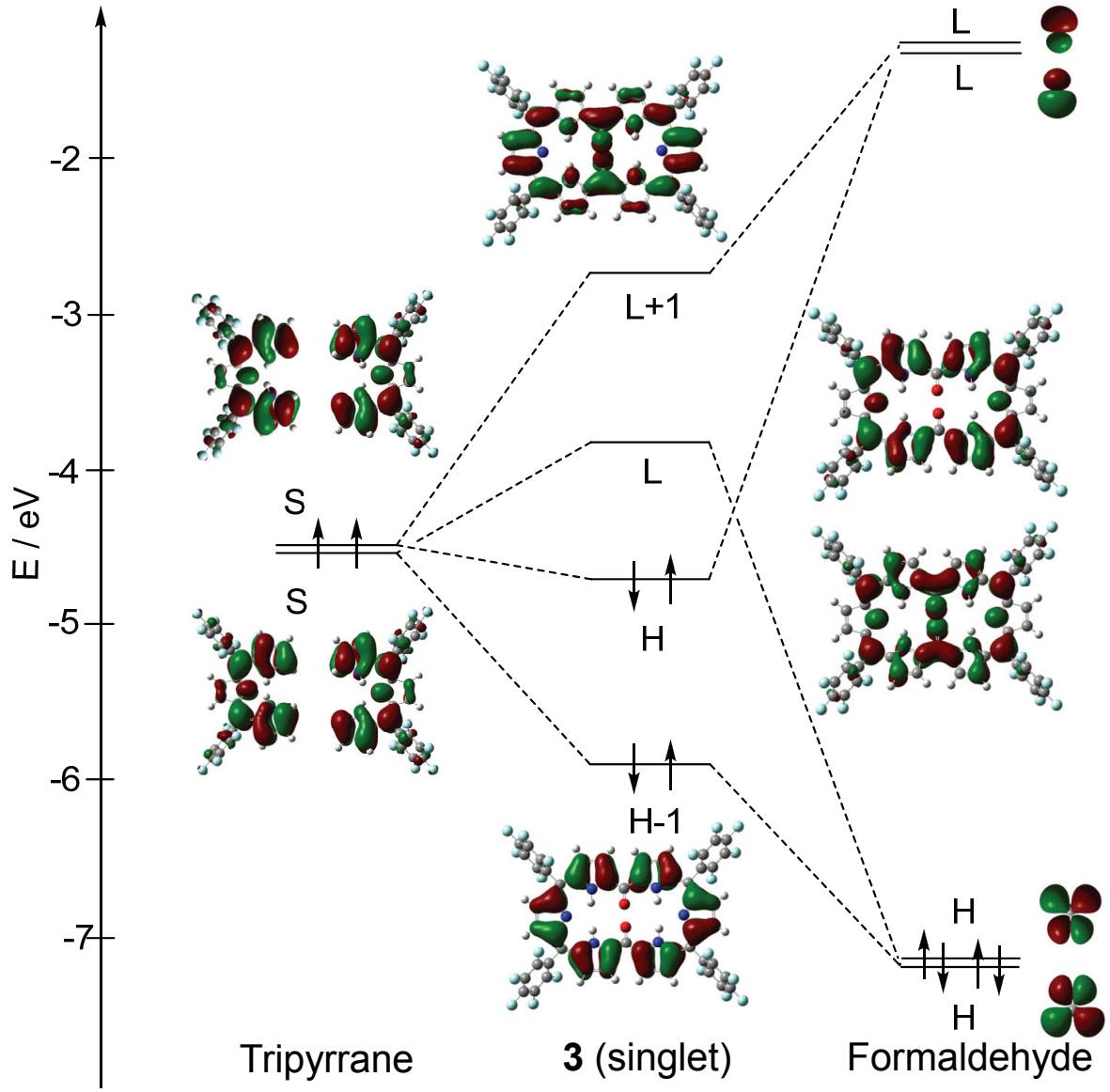

Figure S13. Orbital correlation diagram for **3**. The frontier orbitals of **3** are shown in the center, and those of two isolated tripyrrane radicals and the formaldehyde linker are shown at both ends, respectively. MOs were calculated using the RB3LYP/6-31G(d, p) method. Symbols H, L, and S represent the HOMO, LUMO and SOMO, respectively.

Full references moved from the main text

[13] Gaussian Frisch, M. J.; Trucks, G. W.; Schlegel, H. B.; Scuseria, G. E.; Robb, M. A.; Cheeseman, J. R.; Montgomery, Jr. J. A.; Vreven, T.; Kudin, K. N.; Burant, J. C.; Millam, J. M.; Iyengar, S. S.; Tomasi, J.; Barone, V.; Mennucci, B.; Cossi, M.; Scalmani, G.; Rega, N.; Petersson, G. A.; Nakatsuji, H.; Hada, M.; Ehara, M.; Toyota, K.; Fukuda, R.; Hasegawa, J.; Ishida, M.; Nakajima, T.; Honda, Y.; Kitao, O.; Nakai, H.; Klene, M.; Li, X.; Knox, J. E.; Hratchian, H. P.; Cross, J. B.; Adamo, C.; Jaramillo, J.; Gomperts, R.; Stratmann, R. E.; Yazyev, O.; Austin, A. J.; Cammi, R.; Pomelli, C.; Ochterski, J. W.; Ayala, P. Y.; Morokuma, K.; Voth, G. S43 A.; Salvador, P.; Dannenberg, J. J.; Zakrzewski, V. G.; Dapprich, S.; Daniels, A. D.; Strain, M. C.; Farkas, O.; Malick, D. K.; Rabuck, A. D.; Raghavachari, K.; Foresman, J. B.; Ortiz, J. V.; Cui, Q.; Baboul, A. G.; Clifford, S.; Cioslowski, J.; Stefanov, B. B.; Liu, G.; Liashenko, A.; Piskorz, P.; Komaromi, I.; Martin, R. L.; Fox, D. J.; Keith, T.; Al-Laham, M. A.; Peng, C. Y.; Nanayakkara, A.; Challacombe, M.; Gill, P. M. W.; Johnson, B.; Chen, W.; Wong, M. W.; Gonzalez, C.; Pople, J. A. Gaussian 03, Revision B.05; Gaussian, Inc.: Pittsburgh, PA, 2003. 03 program.

[15] Ohta, S.; Nakano, M.; Kubo, T.; Kamada, K.; Ohta, K.; Kishi, R.; Nakagawa, N.; Champagen, B.; Botek, E.; Takebe, A.; Umezaki, S.; Nate, M.; Takahashi, H,; Furukawa, S.; Morita, Y.; Nakasuji, K.; Yamaguchi, K. *J. Phys, Chem. A* **2007**, 111, 3633.

[26] (a) Ohta, S.; Nakano, M.; Kubo, T.; Kamada, K.; Ohta, K.; Kishi, R.; Nakagawa, N.; Champagne, B.; Botek, E.; Umezaki, S.; Takebe, A.; Takahashi, H.; Furukawa, S.; Morita, Y.; Nakasuji, K.; Yamaguchi, K. *Chem. Phys. Lett*. **2006**, *420*, 432. (b) Nakano, M.; Nakagawa, N.; Kishi, R.; Ohta, S.; Nate, M.; Takahashi, H.; Kubo, T.; Kamada, K.; Ohta, K.; Champagne, B.; Botek, E.; Morita, Y.; Nakasuji, K.; Yamaguchi, K. *J. Phys. Chem. A* **2007**, *111*, 9102. (c) Nakano, M.; Minami, T.; Yoneda, K.; Muhammad, S.; Kishi, R.; Shigeta, Y.; Kubo, T.; Rougier, L.; Champagne, B.; Kamada, K.; Ohta, K. *J. Phys. Chem. Lett.* **2011**, *2*, 1094.